APPENDIX A

HALL EFFECT MEASUREMENTS

Contents:

A.1 GENERAL

The model Hall effect system consists of a uniform slab of electrically conducting material through which a uniform current density flows in the presence of a perpendicular applied magnetic field. The Lorentz force deflects moving charge carriers to one side of the sample and generates an electric field perpendicular to both the current density and the applied magnetic field. The Hall coefficient is the ratio of the perpendicular electric field to the product of current density and magnetic field, while the resistivity is the ratio of the parallel electric field to the current density

Experimental determination of a real material's transport properties requires some significant departures from the ideal model. To begin with, one cannot directly measure the electric field or current density inside a sample. Current density is determined from the total excitation current and the sample's geometry. Electric fields are determined by measuring voltage differences between electrical contacts on the sample surface.

Electrical contacts are made of conductive material, and usually have a higher conductivity than the sample material itself. Electric current therefore tends to flow through the contacts rather than the sample, distorting the current density and electric field in the sample from the ideal. Excitation current flowing through the contacts used to measure voltage differences reduces both current density in the vicinity and the Hall field. If a contact extends across the sample in the same direction as the Hall field, it can conduct current from one side of the sample to the other, shorting out the Hall voltage and leading to an underestimate of the Hall coefficient. Finally, if pairs of contacts used in a voltage measurement are not aligned properly either perpendicular or parallel to the excitation current density, then the voltages measured will not correctly determine the perpendicular or parallel component of the electric field. To minimize these geometrical problems, one must take care with the size and placement of electrical contacts to the sample.

There are also many intrinsic physical mechanisms that alter current density and electric field behavior in a real material. Most of these relate to the thermoelectric behavior of the material in or out of a magnetic field. Some of these effects can be minimized by controlling temperature in the sample's vicinity to minimize thermal gradients across it. In addition, most errors introduced by intrinsic physical mechanisms can be canceled by reversing either the excitation current or the magnetic field and averaging measurements.

A.2 HALL EFFECT MEASUREMENT THEORY

Hall effect measurements commonly use two sample geometries: (1) long, narrow Hall bar geometries and (2) nearly square or circular van der Pauw geometries. Each has advantages and disadvantages. In both types of samples, a Hall voltage is developed perpendicular to a current and an applied magnetic flux. The following is an introduction to the Hall effect and its use in materials characterization. A number of other sources are available for further information[1,2,3,4].

Hall bar geometry: Some common Hall bar geometries are shown in Figure A-1. The Hall voltage developed across an 8-contact Hall bar sample with contacts numbered as in Figure A-1 is:

$$V_H = V_{24} = \frac{R_H B I}{t}$$

where V_{24} is the voltage measured between the opposing contacts numbered 2 and 4, R_H is the Hall coefficient of the material, *B* is the applied magnetic flux density, *I* is the current, and *t* is the thickness of the sample (in the direction parallel to *B*). This section assumes SI units. For a given material, increase the Hall voltage by increasing *B* and *I* and by decreasing sample thickness.

The relationship between the Hall coefficient and the type and density of charge carriers can be complex, but useful insight can be developed by examining the limit $B \rightarrow \infty$, when:

$$R_H = \frac{r}{q(p-n)}$$

where *r* is the Hall scattering factor, *q* is the fundamental electric charge, *p* is the density of positive and *n* the density of negative charge carriers in the material. For the case of a material with one dominant carrier, the Hall coefficient is inversely proportional to the carrier density. The measurement implication is that the greater the density of dominant charge carriers, the smaller the Hall coefficient and the smaller the Hall voltage which must be measured. The scattering factor *r* depends on the scattering mechanisms in the material and typically lies between 1 and 2.[1,5]

Another quantity frequently of interest is the carrier mobility, defined as: $\mu_H = \frac{|R_H|}{\rho}$

where μ_H is the Hall mobility and ρ is the electrical resistivity at zero magnetic flux density. The electrical resistivity can be measured by applying a current between contacts 5 and 6 of the sample shown in Figure A-1 and measuring the voltage between contacts 1 and 3, then using the formula:

$$\rho(B) = \frac{V_{13}}{I_{56}} \frac{wt}{b}$$

where *w* is the width and *t* is the thickness of the Hall bar, *b* is the distance between contacts 1-3, and *B* is the magnetic flux density at which the measurement is taken. The Hall bar is a good geometry for making resistance measurements since about half of the voltage applied across the sample appears between the voltage measurement contacts. For this reason, Hall bars of similar geometries are commonly used when measuring magnetoresistance or Hall mobility on samples with low resistances.

Disadvantages of Hall bar geometries include the following: A minimum of six contacts to make mobility measurements; accuracy of resistivity measurements is sensitive to the geometry of the sample; Hall bar width and the distance between the side contacts can be especially difficult to measure accurately. The accuracy can be increased by making contact to the sides of the bar at the end of extended arms as shown in Figure A-2. Creating such patterns can be difficult and can result in fragile samples.

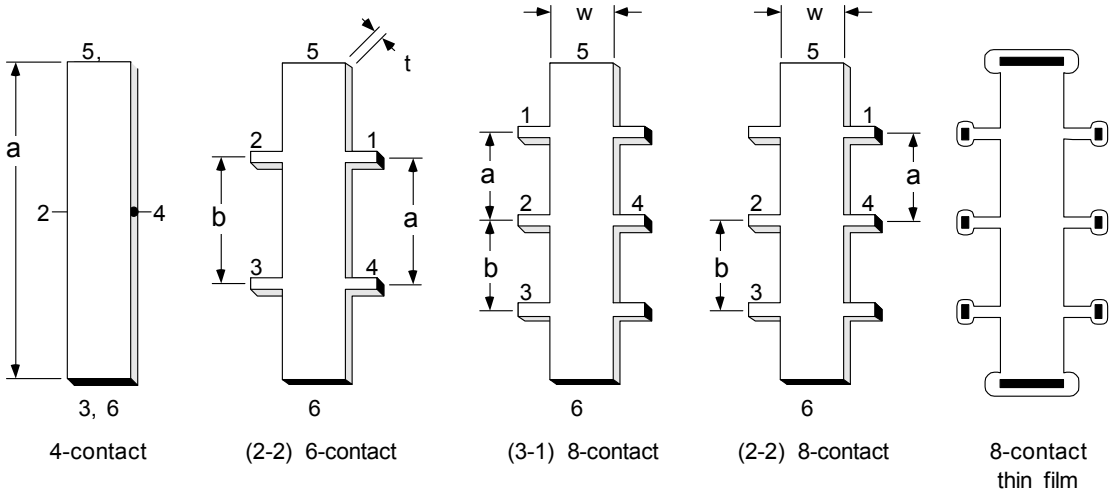

Figure A-1 Common Hall Bar Geometries. Sample thickness, t, of a thin film sample = diffusion depth or layer thickness. Contacts are black, numbered according to the standard to mount in Lake Shore sample holders.

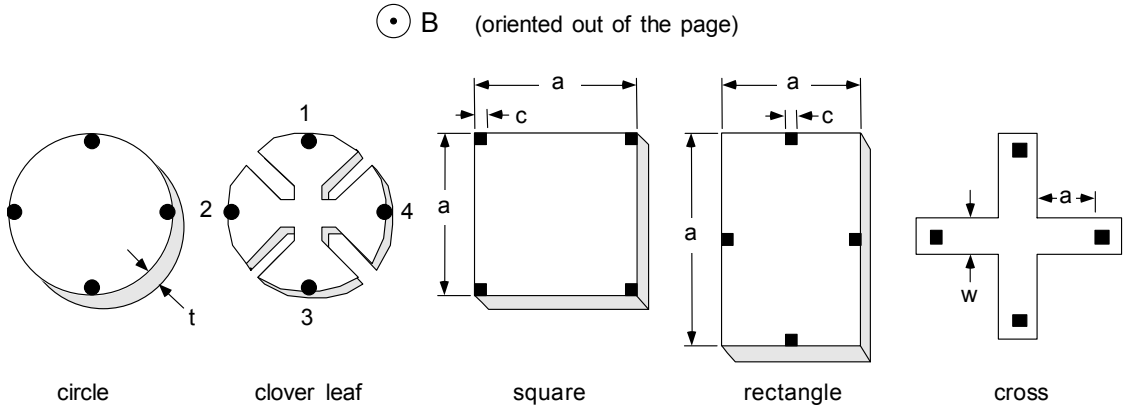

Figure A-2 Common van der Pauw Sample Geometries. The cross appears as a thin film pattern and the others are bulk samples. Contacts are black.

van der Pauw geometry: Some disadvantages of Hall bar geometries can be avoided with van der Pauw sample geometries (see Figure A-2). Van der Pauw [5,6] showed how to calculate the resistivity, carrier concentration, and mobility of an arbitrary, flat sample if the following conditions are met:

1. The contacts are on the circumference of the sample.
2. The contacts are sufficiently small.
3. The sample is of uniform thickness, and:
4. The sample is singly connected (contains no isolated holes).

The resistivity of a van der Pauw sample is given by the expression:

$$\rho = \frac{\pi t}{\ln(2)} \frac{V_{43}}{I_{12}} + \frac{V_{14}}{I_{23}}$$

where V_{23} is defined as V_2 - V_3 and I_{12} indicates the current enters the sample through contact 1 and leaves through contact 2. Two voltage readings are required with the van der Pauw sample, whereas the resistivity measurement on a Hall bar requires only one. This same requirement applies to Hall coefficient measurement as well, so equivalent measurements take twice as long with van der Pauw samples.

The quantity F is a transcendental function of the ratio R_r, defined as:

$$R_r \equiv \frac{V_{43}}{I_{12}} \frac{I_{23}}{V_{14}} \equiv \frac{R_{12,43}}{R_{23,14}} \text{ or } R_r \equiv \frac{I_{12}}{V_{43}} \frac{V_{14}}{I_{23}} \equiv \frac{R_{23,14}}{R_{12,43}}$$

whichever is **greater**, and F is found by solving the equation:

$$\frac{R_r - 1}{R_r + 1} = \frac{F}{\ln(2)} \operatorname{arcosh}\left\{\frac{\exp[\ln(2)/F]}{2}\right\}$$

F=1 when R_r=1, which occurs with symmetrical samples like circles or squares when the contacts are equally spaced and symmetrical. The best measurement accuracy is also obtained when R_r =1.

Squares and circles are the most common van der Pauw geometries, but contact size and placement can significantly effect measurement accuracy. A few simple cases were treated by van der Pauw. Others have shown that for square samples with sides of length *a* and square or triangular contacts of size δ in the four corners, if $\delta/a < 0.1$, then the measurement error is less than 10%[6]. The error is reduced by placing the contacts on square samples at the midpoint of the sides rather than in the corners[7]. The Greek cross shown in Figure A-2 has arms which serve to isolate the contacts from the active region. When using the Greek cross sample geometry with a/w > 1.02, less than 1% error is introduced[8]. A cloverleaf shaped structure like the one shown in Figure A-2 is often used for a patternable thin film on a substrate. The active area in the center is connected by four pathways to four connection pads around its perimeter. This shape makes the measurement much less sensitive to contact size, allowing for larger contact areas.

The contact size affects voltage required to pass a current between two contacts. Ideal point contacts would produce no error due to contact size, but require an enormous voltage to force the current through the infinitesimal contact area. Even with square contacts in the corners of a square sample with $\delta/a < 0.1$, the ratio of the output to input voltage V_{43}, V_{12} is on the order of 1/10. Van der Pauw sample geometries are thus much less efficient at using the available excitation voltage than Hall bars.

Advantages of van der Pauw samples: Only four contacts required. No need to measure sample widths or distances between contacts. Simple geometries can be used.

Disadvantages: Measurements take about twice as long. Errors due to contact size and placement can be significant when using simple geometries.

Mobility spectra: Hall effect measurements are usually performed at just one magnetic flux density, although polarity is reversed and the voltage readings averaged to remove some sources or error. The resulting single mobility calculated from the measurements is a weighted average of the mobilities of all carriers present in the sample. Beck and Anderson[9] developed a technique for interpreting magnetic flux-dependent Hall data which generates a mobility spectrum. The result is a plot of the carrier concentration of conductivity as a function of the mobility. The number of peaks appearing in a mobility spectrum indicates the number of distinct charge carriers active in the material. This powerful technique has virtually eliminated the need for destructive testing techniques such as differential profiling. An example mobility spectrum analysis performed on a GaAs/AlGaAs five-quantum-well heterostructure is shown in Figure 2-9 of their paper.

A technique combining mobility spectrum analysis and multi-carrier fitting was developed by Brugger and Kosser[10], yielding some improvement. The development of quantitative mobility spectrum analysis by Antoszewski et al.[2,11,12,13] has produced even greater improvements in capability.

A.3 SAMPLE GEOMETRIES AND MEASUREMENTS SUPPORTED BY IDEAS HALL SOFTWARE

This section describes common sample geometries useful in Lake Shore's 9500 Series Hall Measurement System and formulas used to calculate resistivities, Hall coefficients, carrier concentrations, and mobilities.

A.3.1 System of Units

Hall effect and magnetoresistance measurements commonly use two systems of units: the SI system and the so-called "laboratory" system. The laboratory system is a hybrid, combining elements of the SI, emu, and esu unit systems. Table A-1 lists the most common quantities, their symbols, their units in both systems, and the conversion factor between them.

Table A- 1 Unit Systems and Conversions

Quantity	Symbol	SI	= Factor x	Laboratory
Capacitance	*C*	farad	1	farad
Carrier concentration	*c,n,p*	m^{-3}	10^{-6}	cm^{-3}
Charge	*q,e*	coulomb	1	coulomb
Conductivity (volume)	σ	(ohm m)-1	10-2	$(ohm\ cm)^{-1}$
Current	*I*	ampere	1	ampere
Current density	*j*	$ampere/m^2$	10^{-4}	$ampere/cm^2$
Electric field intensity	*E*	volt/m	10^{-2}	volt/cm
Hall coefficient	R_H	m^3/coulomb	10^6	cm^3/coulomb
Magnetic induction	*B*	tesla (= V s/m2)	10^4	gauss
Mobility	μ_H	m^2/V s	10^4	cm^2/V s
Electric potential	*V*	volt	1	volt
Resistivity	ρ	ohm m	10^2	ohm cm

To use this table, 1 SI unit = (factor) x 1 laboratory unit. For example, 1 tesla = 10^4 gauss.

A.3.2 Nomenclature

The equations below appear twice - once in SI units, once in laboratory units. In all cases, voltages are measured in volts, electric currents are measured in amperes, and resistances are measured in ohms. All other measured quantities appear with their respective unit in brackets. For example, the width of a sample in SI units appears as $w[m]$. The equations below indicate voltages and currents as follows:

VOLTAGE NOMENCLATURE

$V^{\pm}_{kl}(\pm B)$ indicates a voltage difference $V_k - V_l$ measured between terminals *k* and *l*. Terminal *i* is connected to the excitation current source and terminal *j* is connected to the current sink.

The superscript ±. Indicates the sign of the excitation current supplied by the current source. ±B indicates the sign of the applied magnetic induction *B*, measured in the direction shown on the drawings.

Example: $V^{-}_{56,12}(+B)$ indicates a voltage difference $V_1 - V_2$ measured while a negative current was supplied by a current source at terminal 5 and flowed to terminal 6, in the presence of a positive applied magnetic induction.

CURRENT NOMENCLATURE

$(\pm B)$ indicates a current flowing from terminal *i* to terminal *j* of polarity given by the superscript ± and with the indicated magnetic field polarity.

A.3.3 Van der Pauw Measurements

The van der Pauw structure is probably the most popular Hall measurement geometry, primarily because it requires fewer geometrical measurements of the sample. In 1958, van der Pauw[13] solved the general problem of the potential in a thin conducting layer of arbitrary shape. His solution allowed Hall and resistivity measurements to be made on any sample of uniform thickness, provided that the sample was homogeneous and there were no holes in it. All that is needed to calculate *sheet* resistivity or carrier concentration is four point contacts on the edge of the surface (or four line contacts on the periphery); an additional measurement of sample thickness allows calculation of *volume* resistivity and carrier concentration. These relaxed requirements on sample shape simplify fabrication and measurement in comparison to Hall bar techniques.

On the other hand, the van der Pauw structure is more susceptible to errors caused by the finite size of the contacts than the Hall bar. It is also impossible to accurately measure magnetoresistance with the van der Pauw geometry, so both Hall effect and magnetoresistance (i.e. the whole conductivity tensor) measurements must be done with a Hall bar geometry.

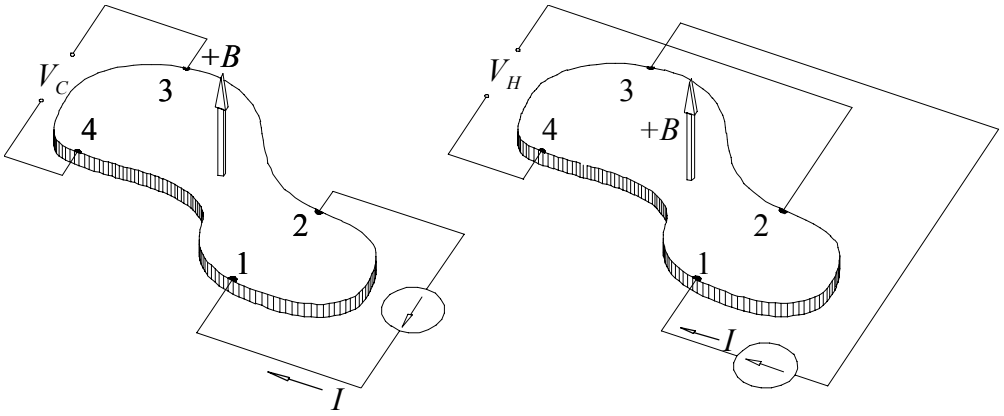

Figure A-3 Measuring Resistivity and Hall Coefficient Using a van der Pauw Geometry.

In the basic van der Pauw contact arrangement, the four contacts made to the sample are numbered counter-clockwise in ascending order when the sample is viewed from above with the magnetic field perpendicular to the sample and pointing toward the observer. The sample interior should contain no contacts or holes. The sample must be homogeneous and of uniform thickness.

Resistivity

Again, let V^{+}_{ijkl} indicate a voltage measured across terminals *k* and *l,* with *k* positive, while a positive current flows into terminal *i* and out of terminal *j*. In a similar fashion, let R^{+}_{ijkl} indicate a resistance $R^{+}_{ijkl} = V_{kl} / I_{ij}$, with the voltage measured across terminals *k* and *l*, while a positive current flows into *i* and out of *j*. First calculate the two resistivities:

$$\rho_A = \frac{\pi f_A \; t[m,cm]}{\ln(2)} \left\{ \frac{V^{+}_{12,43} - V^{-}_{12,43} + V^{+}_{23,14} - V^{-}_{23,14}}{I^{+}_{12} - I^{-}_{12} + I^{+}_{23} - I^{-}_{23}} \right\} \quad [\Omega \cdot \mathrm{m}, \Omega \cdot \mathrm{cm}],$$

and

$$\rho_B = \frac{\pi f_B \; t[m,cm]}{\ln(2)} \left\{ \frac{V^{+}_{34,21} - V^{-}_{34,21} + V^{+}_{41,23} - V^{-}_{41,23}}{I^{+}_{34} - I^{-}_{34} + I^{+}_{41} - I^{-}_{41}} \right\} \quad [\Omega \cdot \mathrm{m}, \Omega \cdot \mathrm{cm}].$$

Geometrical factors f_A and f_B are functions of resistance ratios Q_A and Q_B, respectively, given by:

$$Q_A = \left(\frac{R^{+}_{12,43} - R^{-}_{12,43}}{R^{+}_{23,14} - R^{-}_{23,14}} \right) = \left(\frac{V^{+}_{12,43} - V^{-}_{12,43}}{I^{+}_{12} - I^{-}_{12}} \right) \left(\frac{I^{+}_{23} - I^{-}_{23}}{V^{+}_{23,14} - V^{-}_{23,14}} \right),$$

and

$$Q_B = \left(\frac{R^{+}_{34,21} - R^{-}_{34,21}}{R^{+}_{41,23} - R^{-}_{41,23}} \right) = \left(\frac{V^{+}_{34,21} - V^{-}_{34,21}}{I^{+}_{34} - I^{-}_{34}} \right) \left(\frac{I^{+}_{41} - I^{-}_{41}}{V^{+}_{41,23} - V^{-}_{41,23}} \right).$$

If either Q_A or Q_B is greater than one, then use the reciprocal instead. The relationship between f and Q is expressed by the transcendental equation

$$\frac{Q-1}{Q+1} = \frac{f}{\ln 2}\cosh^{-1}\left\{\frac{1}{2}\exp\left[\frac{\ln 2}{f}\right]\right\},$$

which can be solved numerically.

The two resistivities ρ_A and ρ_B should agree to within ±10%. If they do not, then the sample is too inhomogeneous, or anisotropic, or has some other problem. If they do agree, the average resistivity is given by

$$\rho_{av} = \frac{\rho_A + \rho_B}{2} \quad [\Omega\cdot\mathrm{m}, \Omega\cdot\mathrm{cm}].$$

Magnetoresistivity

If desired, calculate the magnetoresistivity as

$$\rho_A(B) = \frac{\pi f_A\ t[m,cm]}{\ln(2)}\left\{\frac{V^+_{12,43}(+B) - V^-_{12,43}(+B) + V^+_{23,41}(+B) - V^-_{23,41}(+B)}{I^+_{12}(+B) - I^-_{12}(+B) + I^+_{23}(+B) - I^-_{23}(+B)}\cdots\right.$$
$$\left.\frac{+V^+_{12,43}(-B) - V^-_{12,43}(-B) + V^+_{23,41}(-B) - V^-_{23,41}(-B)}{+I^+_{12}(-B) - I^-_{12}(-B) + I^+_{23}(-B) - I^-_{23}(-B)}\right\} \quad [\Omega\cdot\mathrm{m}, \Omega\cdot\mathrm{cm}],$$

and

$$\rho_B(B) = \frac{\pi f_B\ t[m,cm]}{\ln(2)}\left\{\frac{V^+_{34,21}(+B) - V^-_{34,21}(+B) + V^+_{41,23}(+B) - V^-_{41,23}(+B)}{I^+_{34}(+B) - I^-_{34}(+B) + I^+_{41}(+B) - I^-_{41}(+B)}\cdots\right.$$
$$\left.\frac{+V^+_{34,21}(-B) - V^-_{34,21}(-B) + V^+_{41,23}(-B) - V^-_{41,23}(-B)}{+I^+_{34}(-B) - I^-_{34}(-B) + I^+_{41}(-B) - I^-_{41}(-B)}\right\} \quad [\Omega\cdot\mathrm{m}, \Omega\cdot\mathrm{cm}].$$

Calculate factors f_A and f_B the same way as at zero magnetic field, and the average magnetoresistivity is:

$$\rho_{av}(B) = \frac{\rho_A(B) + \rho_B(B)}{2} \quad [\Omega\cdot\mathrm{m}], [\Omega\cdot\mathrm{cm}].$$

This measurement does not give the true magnetoresistance, as defined in terms of the material's conductivity tensor. Van der Pauw's calculation of resistivity is invalid in the presence of a magnetic field, since the magnetic field alters the current density vector field inside the sample. On the other hand, magnetoresistance measurements are routinely performed on van der Pauw samples anyway.

Hall Coefficient

Calculate two values of the Hall coefficient by the following:

$$R_{HC} = \frac{t[\mathrm{m}]}{B[\mathrm{T}]} \frac{V^{+}_{31,42}(+B) - V^{-}_{31,42}(+B) + V^{-}_{31,42}(-B) - V^{+}_{31,42}(-B)}{I^{+}_{31}(+B) - I^{-}_{31}(+B) + I^{-}_{31}(-B) - I^{+}_{31}(-B)} \quad \left[\mathrm{m}^3 \cdot C^{-1}\right]$$

$$= 10^8 \frac{t[\mathrm{cm}]}{B[\mathrm{gauss}]} \frac{V^{+}_{31,42}(+B) - V^{-}_{31,42}(+B) + V^{-}_{31,42}(-B) - V^{+}_{31,42}(-B)}{I^{+}_{31}(+B) - I^{-}_{31}(+B) + I^{-}_{31}(-B) - I^{+}_{31}(-B)} \quad \left[\mathrm{cm}^3 \cdot C^{-1}\right],$$

and

$$R_{HD} = \frac{t[\mathrm{m}]}{B[\mathrm{T}]} \frac{V^{+}_{42,13}(+B) - V^{-}_{42,13}(+B) + V^{-}_{42,13}(-B) - V^{+}_{42,13}(-B)}{I^{+}_{42}(+B) - I^{-}_{42}(+B) + I^{-}_{42}(-B) - I^{+}_{42}(-B)} \quad \left[\mathrm{m}^3 \cdot \mathrm{C}^{-1}\right]$$

$$= 10^8 \frac{t[\mathrm{cm}]}{B[\mathrm{gauss}]} \frac{V^{+}_{42,13}(+B) - V^{-}_{42,13}(+B) + V^{-}_{42,13}(-B) - V^{+}_{42,13}(-B)}{I^{+}_{42}(+B) - I^{-}_{42}(+B) + I^{-}_{42}(-B) - I^{+}_{42}(-B)} \quad \left[\mathrm{cm}^3 \cdot \mathrm{C}^{-1}\right].$$

These two should agree to within ±10%. If they do not, then the sample is too inhomogeneous, or anisotropic, or has some other problem. If they do, then the average Hall coefficient can be calculated by

$$R_{Hav} = \frac{R_{HC} + R_{HD}}{2} \quad \left[\mathrm{m}^3 \cdot \mathrm{C}^{-1}, \mathrm{cm}^3 \cdot \mathrm{C}^{-1}\right]$$

Hall Mobility

The Hall mobility is given by

$$\mu_H = \frac{|R_{Hav}|}{\rho_{av}} \quad \left[\mathrm{m}^2 \cdot \mathrm{V}^{-1} \cdot \mathrm{s}^{-1}, \mathrm{cm}^2 \cdot \mathrm{V}^{-1} \cdot \mathrm{s}^{-1}\right],$$

where ρ_{av} is the magnetoresistivity if it was measured, and the zero-field resistivity if it was not.

A.3.4 Hall Bar Measurements

Hall bars approximate the ideal geometry for measuring the Hall effect, in which a constant current density flows along the long axis of a rectangular solid, perpendicular to an applied external magnetic field.

A.3.4.1 Six-contact 1-2-2-1 Hall Bar

An ideal six-contact 1-2-2-1 Hall bar geometry is symmetrical. Contact separations *a* and *b* on either side of the sample are equal, with contacts located opposite one another. Contact pairs are placed symmetrically about the midpoint of the sample's long axis.

This geometry allows two equivalent measurement sets to check for sample homogeneity in both resistivity and Hall coefficient. However, the close location of the Hall voltage contacts to the sample ends may cause the end contacts to short out the Hall voltage, leading to an underestimate of the actual Hall coefficient. While the 1-2-2-1 Hall bar geometry is included in ASTM Standard F76, the contact numbering given here differs from the standard.

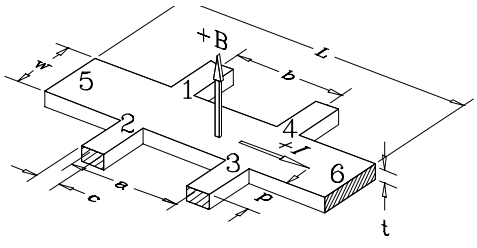

Figure A-4 Six-Contact 1-2-2-1 Hall Bar Geometry

Resistivity

To calculate resistivity at zero field, first calculate

$$\rho_A = \frac{V^+_{56,23}(B=0) - V^-_{56,23}(B=0)}{I^+_{56}(B=0) - I^-_{56}(B=0)} \frac{w[\mathrm{m}]\, t[\mathrm{m}]}{a[\mathrm{m}]} \quad [\Omega \cdot \mathrm{m}]$$

$$= \frac{V^+_{56,23}(B=0) - V^-_{56,23}(B=0)}{I^+_{56}(B=0) - I^-_{56}(B=0)} \frac{w[\mathrm{cm}]\, t[\mathrm{cm}]}{a[\mathrm{cm}]} \quad [\Omega \cdot \mathrm{cm}],$$

and

$$\rho_B = \frac{V^+_{56,14}(B=0) - V^-_{56,14}(B=0)}{I^+_{56}(B=0) - I^-_{56}(B=0)} \frac{w[\mathrm{m}]\, t[\mathrm{m}]}{b[\mathrm{m}]} \quad [\Omega \cdot \mathrm{m}]$$

$$= \frac{V^+_{56,14}(B=0) - V^-_{56,14}(B=0)}{I^+_{56}(B=0) - I^-_{56}(B=0)} \frac{w[\mathrm{cm}]\, t[\mathrm{cm}]}{b[\mathrm{cm}]} \quad [\Omega \cdot \mathrm{cm}].$$

These two resistivities should agree to within ±10%. If they do not, then the sample is too inhomogeneous, or anisotropic, or has some other problem. If they do, then the average resistivity is given by

$$\rho_{av} = \frac{\rho_A + \rho_B}{2} \quad [\Omega \cdot \mathrm{m}, \Omega \cdot \mathrm{cm}] \ .$$

Magnetoresistivity

Magnetoresistivity is typically used in mobility spectrum calculations, but not in Hall mobility calculations. To calculate magnetoresistivity, first calculate

$$\rho_A(B) = \frac{V^+_{56,23}(+B) - V^-_{56,23}(+B) + V^+_{56,23}(-B) - V^-_{56,23}(-B)}{I^+_{56}(+B) - I^-_{56}(+B) + I^+_{56}(-B) - I^-_{56}(-B)} \frac{w[\mathrm{m}]\, t[\mathrm{m}]}{a[\mathrm{m}]} \quad [\Omega \cdot \mathrm{m}]$$

$$= \frac{V^+_{56,23}(+B) - V^-_{56,23}(+B) + V^+_{56,23}(-B) - V^-_{56,23}(-B)}{I^+_{56}(+B) - I^-_{56}(+B) + I^+_{56}(-B) - I^-_{56}(-B)} \frac{w[\mathrm{cm}]\, t[\mathrm{cm}]}{a[\mathrm{cm}]} \quad [\Omega \cdot \mathrm{cm}],$$

and

$$\rho_B(B) = \frac{V^+_{56,14}(+B) - V^-_{56,14}(+B) + V^+_{56,14}(-B) - V^-_{56,14}(-B)}{I^+_{56}(+B) - I^-_{56}(+B) + I^+_{56}(-B) - I^-_{56}(-B)} \frac{w[\mathrm{m}]\, t[\mathrm{m}]}{b[\mathrm{m}]} \quad [\Omega \cdot \mathrm{m}]$$

$$= \frac{V^+_{56,14}(+B) - V^-_{56,14}(+B) + V^+_{56,14}(-B) - V^-_{56,14}(-B)}{I^+_{56}(+B) - I^-_{56}(+B) + I^+_{56}(-B) - I^-_{56}(-B)} \frac{w[\mathrm{cm}]\, t[\mathrm{cm}]}{b[\mathrm{cm}]} \quad [\Omega \cdot \mathrm{cm}].$$

These two resistivities should agree to within ±10%. If they do not, then the sample is too inhomogeneous, or anisotropic, or has some other problem. If they do, then the average magnetoresistivity is given by

$$\rho_{av}(B) = \frac{\rho_A(B) + \rho_B(B)}{2} \quad [\Omega \cdot \mathrm{m}, \Omega \cdot \mathrm{cm}].$$

Hall Coefficient

First, calculate the individual Hall coefficients

$$R_{HA} = \frac{t[\mathrm{m}]}{B[\mathrm{T}]} \frac{V^{+}_{56,34}(+B) - V^{-}_{56,34}(+B) + V^{-}_{56,34}(-B) - V^{+}_{56,34}(-B)}{I^{+}_{56}(+B) - I^{-}_{56}(+B) + I^{-}_{56}(-B) - I^{+}_{56}(-B)} \quad \left[\mathrm{m}^3 \cdot C^{-1}\right]$$

$$= 10^8 \frac{t[\mathrm{cm}]}{B[\mathrm{gauss}]} \frac{V^{+}_{56,34}(+B) - V^{-}_{56,34}(+B) + V^{-}_{56,34}(-B) - V^{+}_{56,34}(-B)}{I^{+}_{56}(+B) - I^{-}_{56}(+B) + I^{-}_{56}(-B) - I^{+}_{56}(-B)} \quad \left[\mathrm{cm}^3 \cdot C^{-1}\right],$$

and

$$R_{HA} = \frac{t[\mathrm{m}]}{B[\mathrm{T}]} \frac{V^{+}_{56,21}(+B) - V^{-}_{56,21}(+B) + V^{-}_{56,21}(-B) - V^{+}_{56,21}(-B)}{I^{+}_{56}(+B) - I^{-}_{56}(+B) + I^{-}_{56}(-B) - I^{+}_{56}(-B)} \quad \left[\mathrm{m}^3 \cdot \mathrm{C}^{-1}\right]$$

$$= 10^8 \frac{t[\mathrm{cm}]}{B[\mathrm{gauss}]} \frac{V^{+}_{56,21}(+B) - V^{-}_{56,21}(+B) + V^{-}_{56,21}(-B) - V^{+}_{56,21}(-B)}{I^{+}_{56}(+B) - I^{-}_{56}(+B) + I^{-}_{56}(-B) - I^{+}_{56}(-B)} \quad \left[\mathrm{cm}^3 \cdot \mathrm{C}^{-1}\right].$$

If R_{HA} and R_{HB} do not agree to within ±10%, then the sample is too inhomogeneous, or anisotropic, or has some other problem. If they do agree, then the average Hall Coefficient is given by

$$R_{Hav} = \frac{R_{HA} + R_{HB}}{2} \quad \left[\mathrm{m}^3 \cdot \mathrm{C}^{-1}, \mathrm{cm}^3 \cdot \mathrm{C}^{-1}\right].$$

Hall Mobility

$\mu_H = \frac{|R_{Hav}|}{\rho_{av}}$ $\left[\mathrm{m}^2 \cdot \mathrm{V}^{-1} \cdot \mathrm{s}^{-1}, \mathrm{cm}^2 \cdot \mathrm{V}^{-1} \cdot \mathrm{s}^{-1}\right]$ gives the Hall mobility where ρ_{av} is the zero-field resistivity.

A.3.4.2 Six-contact 1-3-1-1 Hall Bar

The ideal 1-3-1-1 Hall bar geometry places contacts 2 and 4 directly across from one another in the exact middle of the sample's length and contacts 1 and 3 symmetrically on either side of contact 2.

This geometry allows no homogeneity checks, but measuring the Hall voltage in the exact center of the sample's length helps minimize the shorting of the Hall voltage via the end contacts. The 1-3-1-1 Hall bar is not included in ASTM Standard F76.

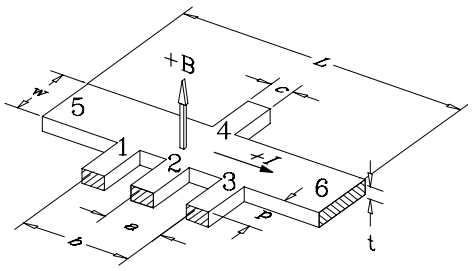

Figure A-5 Six-Contact 1-3-1-1 Hall Bar Geometry

Resistivity

Calculate the resistivity at zero field by

$$\rho = \frac{V^{+}_{56,13}(B=0) - V^{-}_{56,13}(B=0)}{I^{+}_{56}(B=0) - I^{-}_{56}(B=0)} \frac{w[\mathrm{m}]\, t[\mathrm{m}]}{b[\mathrm{m}]} \quad [\Omega \cdot \mathrm{m}]$$

$$= \frac{V^{+}_{56,13}(B=0) - V^{-}_{56,13}(B=0)}{I^{+}_{56}(B=0) - I^{-}_{56}(B=0)} \frac{w[\mathrm{cm}]\, t[\mathrm{cm}]}{b[\mathrm{cm}]} \quad [\Omega \cdot \mathrm{cm}].$$

Magnetoresistivity

If desired, calculate the magnetoresistivity by

$$\rho(B) = \frac{V^{+}_{56,13}(+B) - V^{-}_{56,13}(+B) + V^{+}_{56,13}(-B) - V^{-}_{56,13}(-B)}{I^{+}_{56}(+B) - I^{-}_{56}(+B) + I^{+}_{56}(-B) - I^{-}_{56}(-B)} \frac{w[\mathrm{m}]\, t[\mathrm{m}]}{b[\mathrm{m}]} \quad [\Omega \cdot \mathrm{m}]$$

$$= \frac{V^{+}_{56,13}(+B) - V^{-}_{56,13}(+B) + V^{+}_{56,13}(-B) - V^{-}_{56,13}(-B)}{I^{+}_{56}(+B) - I^{-}_{56}(+B) + I^{+}_{56}(-B) - I^{-}_{56}(-B)} \frac{w[\mathrm{cm}]\, t[\mathrm{cm}]}{b[\mathrm{cm}]} \quad [\Omega \cdot \mathrm{cm}].$$

Hall Coefficient

Calculate the Hall coefficient by

$$R_H = \frac{t[\mathrm{m}]}{B[\mathrm{T}]} \frac{V^{+}_{56,24}(+B) - V^{-}_{56,24}(+B) + V^{-}_{56,24}(-B) - V^{+}_{56,24}(-B)}{I^{+}_{56}(+B) - I^{-}_{56}(+B) + I^{-}_{56}(-B) - I^{+}_{56}(-B)} \quad [\mathrm{m}^3 \cdot \mathrm{C}^{-1}]$$

$$= 10^8 \frac{t[\mathrm{cm}]}{B[\mathrm{gauss}]} \frac{V^{+}_{56,24}(+B) - V^{-}_{56,24}(+B) + V^{-}_{56,24}(-B) - V^{+}_{56,24}(-B)}{I^{+}_{56}(+B) - I^{-}_{56}(+B) + I^{-}_{56}(-B) - I^{+}_{56}(-B)} \quad [\mathrm{cm}^3 \cdot \mathrm{C}^{-1}].$$

Hall Mobility

The Hall mobility is given by $\mu_H = \frac{|R_H|}{\rho} \quad [\mathrm{m}^2 \cdot \mathrm{V}^{-1} \cdot \mathrm{s}^{-1}, \mathrm{cm}^2 \cdot \mathrm{V}^{-1} \cdot \mathrm{s}^{-1}]$,

where ρ is the magnetoresistivity if it was measured, and the zero-field resistivity if it was not.

A.3.4.3 Eight-contact 1-3-3-1 Hall Bar

The eight contact 1-3-3-1 Hall bar geometry is ideally the most symmetrical of the Hall bars. Two sets of three equally-spaced contacts lie directly opposite one another on either side of the sample with center contacts (numbers 2 and 4) located at the exact center of the sample's length. Voltage measurement connections are made to contacts 1 through 4, while current flows from contact 5 to contact 6. Only six of the eight contacts are used in this measuring procedure. The remaining two (unnumbered) contacts are included to keep the sample completely symmetrical.

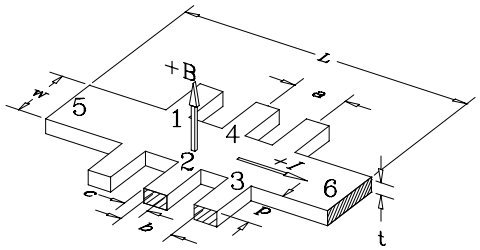

Figure A-6 Eight-Contact 1-3-3-1 Hall Bar Geometry

The eight-contact Hall bar attempts to combine the homogeneity checks possible with the 1-2-2-1 six-contact geometry and the benefit of measuring the Hall voltage in the center of the sample. It allows two resistivity measurements compare for homogeneity, but only one Hall voltage measurement. Either the 1-2-2-1 or 1-3-3-1 six-contact measurements can be made using an eight-contact Hall bar, simply by moving the electrical connections to the appropriate points. The eight-contact Hall bar geometry is included in ASTM Standard F76, but the contact numbering given here differs from the standard.

Resistivity

First calculate the two resistivities

$$\rho_A = \frac{V^+_{56,23}(B=0) - V^-_{56,23}(B=0)}{I^+_{56}(B=0) - I^-_{56}(B=0)} \frac{w[\mathrm{m}]\, t[\mathrm{m}]}{b[\mathrm{m}]} \quad [\Omega \cdot \mathrm{m}]$$

$$= \frac{V^+_{56,23}(B=0) - V^-_{56,23}(B=0)}{I^+_{56}(B=0) - I^-_{56}(B=0)} \frac{w[\mathrm{cm}]\, t[\mathrm{cm}]}{b[\mathrm{cm}]} \quad [\Omega \cdot \mathrm{cm}],$$

and

$$\rho_B = \frac{V^+_{56,14}(B=0) - V^-_{56,14}(B=0)}{I^+_{56}(B=0) - I^-_{56}(B=0)} \frac{w[\mathrm{m}]\, t[\mathrm{m}]}{b[\mathrm{m}]} \quad [\Omega \cdot \mathrm{m}]$$

$$= \frac{V^+_{56,14}(B=0) - V^-_{56,14}(B=0)}{I^+_{56}(B=0) - I^-_{56}(B=0)} \frac{w[\mathrm{cm}]\, t[\mathrm{cm}]}{b[\mathrm{cm}]} \quad [\Omega \cdot \mathrm{cm}]$$

at zero magnetic field.

If these two values disagree by more than ±10%, then the sample is too inhomogeneous, or anisotropic, or has some other problem. If they do agree, then the average resistivity is given by

$$\rho_{av} = \frac{\rho_A + \rho_B}{2} \quad [\Omega \cdot \mathrm{m}], [\Omega \cdot \mathrm{cm}] \ .$$

Magnetoresistivity

If desired, calculate the two magnetoresistivities

$$\rho_A = \frac{V^+_{56,23}(+B) - V^-_{56,23}(+B) + V^+_{56,23}(-B) - V^-_{56,23}(-B)}{I^+_{56}(+B) - I^-_{56}(+B) + I^+_{56}(-B) - I^-_{56}(-B)} \frac{w[\mathrm{m}]\, t[\mathrm{m}]}{b[\mathrm{m}]} \quad [\Omega \cdot \mathrm{m}]$$

$$= \frac{V^+_{56,23}(+B) - V^-_{56,23}(+B) + V^+_{56,23}(-B) - V^-_{56,23}(-B)}{I^+_{56}(+B) - I^-_{56}(+B) + I^+_{56}(-B) - I^-_{56}(-B)} \frac{w[\mathrm{cm}]\, t[\mathrm{cm}]}{b[\mathrm{cm}]} \quad [\Omega \cdot \mathrm{cm}],$$

and

$$\rho_B = \frac{V^+_{56,14}(+B) - V^-_{56,14}(+B) + V^+_{56,14}(-B) - V^-_{56,14}(-B)}{I^+_{56}(+B) - I^-_{56}(+B) + I^+_{56}(-B) - I^-_{56}(-B)} \frac{w[\mathrm{m}]\, t[\mathrm{m}]}{b[\mathrm{m}]} \quad [\Omega \cdot \mathrm{m}]$$

$$= \frac{V^+_{56,14}(+B) - V^-_{56,14}(+B) + V^+_{56,14}(-B) - V^-_{56,14}(-B)}{I^+_{56}(+B) - I^-_{56}(+B) + I^+_{56}(-B) - I^-_{56}(-B)} \frac{w[\mathrm{cm}]\, t[\mathrm{cm}]}{b[\mathrm{cm}]} \quad [\Omega \cdot \mathrm{cm}].$$

If these two values disagree by more than ±10%, then the sample is too inhomogeneous, or anisotropic, or has some other problem. If they do agree, then the average magnetoresistivity is given by

$$\rho_{av}(B) = \frac{\rho_A(B) + \rho_B(B)}{2} \quad [\Omega \cdot \mathrm{m}, \Omega \cdot \mathrm{cm}] .$$

Hall Coefficient

Calculate the Hall coefficient by

$$R_H = \frac{t[\mathrm{m}]}{B[\mathrm{T}]} \frac{V^+_{56,24}(+B) - V^-_{56,24}(+B) + V^-_{56,24}(-B) - V^+_{56,24}(-B)}{I^+_{56}(+B) - I^-_{56}(+B) + I^-_{56}(-B) - I^+_{56}(-B)} \quad \left[\mathrm{m}^3 \cdot \mathrm{C}^{-1}\right]$$

$$= 10^8 \frac{t[\mathrm{cm}]}{B[\mathrm{gauss}]} \frac{V^+_{56,24}(+B) - V^-_{56,24}(+B) + V^-_{56,24}(-B) - V^+_{56,24}(-B)}{I^+_{56}(+B) - I^-_{56}(+B) + I^-_{56}(-B) - I^+_{56}(-B)} \quad \left[\mathrm{cm}^3 \cdot \mathrm{C}^{-1}\right].$$

Hall Mobility

The Hall mobility is given by

$$\mu_H = \frac{|R_{Hav}|}{\rho_{av}} \quad \left[\mathrm{m}^2 \cdot \mathrm{V}^{-1} \cdot \mathrm{s}^{-1}, \mathrm{cm}^2 \cdot \mathrm{V}^{-1} \cdot \mathrm{s}^{-1}\right],$$

where ρ_{av} is the magnetoresistivity if it was measured, and the zero-field resistivity if it was not.

A.4 COMPARISON TO ASTM STANDARD

The contact numbering and voltage measurement indexing given above differ in several ways from that given in the ASTM Standard F76[15].

To begin, the ASTM contact numbering schemes for the van der Pauw and Hall Bar geometries are incompatible with one another. To allow either sample type to be mounted using the same set of contacts, Lake Shore's numbering scheme for Hall bar samples differs from the ASTM scheme.

Second, the ASTM standard is inconsistent with the "handedness" of the van der Pauw contact numbering order with respect to the applied magnetic field. Lake Shore numbered the contacts counter-clockwise in ascending order when the sample is viewed from above with the magnetic field perpendicular to the sample and pointing toward the observer, as shown in Figure A-3 **Measuring Resistivity and Hall Coefficient Using a van der Pauw Geometry.**

Finally, the ASTM assumes that the direction of the excitation current is to be changed by physically reversing the current connections. This technique is not well suited to high-resistance samples using a programmable current source like the Keithley Model 220. This current source (and others like it) has a guarded "high" current output, and an unguarded "low" current return. For proper current source operation, the "high" output lead should be farther from common ground than the "low" return lead, a condition violated half of the time when physically reversing the high and low current leads to the sample. When this condition is violated, leakage current can flow through the voltmeter, leading to possibly serious measurement errors.

To avoid this difficulty, Lake Shore reversed the sign of the programmed current source, while leaving the contacts alone. This requires a more sophisticated notation for voltage measurements:

$$V^{\pm}_{ij,kl}(\pm B)$$

In this notation, terminal i refers to the contact to which the current source output attaches, terminal j is the current return contact, terminal k is the positive voltmeter terminal, and terminal l is the negative voltmeter terminal. The superscript ± refers to the sign of the programmed current, while $\pm B$ refers to the sign of the applied magnetic field relative to the positive direction indicated in the figures.

A.5 SOURCES OF MEASUREMENT ERROR

David C. Look gives a good treatment of systematic error sources in Hall effect measurements in the first chapter of his book.[2] There are two kinds of error sources: intrinsic and geometrical.

A.5.1 Intrinsic Error Sources

The apparent Hall voltage, V_{Ha}, measured with a single reading can include several spurious voltages. These spurious error sources include the following:

1. **Voltmeter offset (V_o):** An improperly zeroed voltmeter adds a voltage V_o to every measurement. The offset does not change with sample current or magnetic field direction.
2. **Current meter offset (I_o):** An improperly zeroed current meter adds a current I_o to every measurement. The offset does not change with sample current or magnetic field direction.
3. **Thermoelectric voltages (V_S):** A temperature gradient across the sample allows two contacts to function as a pair of thermocouple junctions. The resulting thermoelectric voltage due to the Seebeck effect is designated V_s. Portions of wiring to the sensor can also produce thermoelectric voltages in response to temperature gradients. These thermoelectric voltages are not affected by current or magnetic field, to first order.
4. **Ettingshausen effect voltage (V_E):** Even if no external transverse temperature gradient exists, the sample can set up its own. The e**v**x**B** force shunts slow (cool) and fast (hot) electrons to the sides in different numbers and causes an internally generated Seebeck effect. This phenomenon is known as the Ettingshausen effect. Unlike the Seebeck effect, V_E is proportional to both current and magnetic field.
5. **Nernst effect voltage (V_N):** If a longitudinal temperature gradient exists across the sample, then electrons tend to diffuse from the hot end of the sample to the cold end and this diffusion current is affected by a magnetic field, producing a Hall voltage. The phenomenon is known as the Nernst or Nernst-Ettingshausen effect. The resulting voltage is designated V_N and is proportional to magnetic field, but not to external current. This is the one intrinsic error source which can not be eliminated from a Hall voltage measurement by field or current reversal.
6. **Righi-Leduc voltage (V_R):** The Nernst (diffusion) electrons also experience an Ettingshausen-type effect since their spread of velocities result in hot and cold sides and thus again set up a transverse Seebeck voltage, known as the Righi-Leduc voltage, V_R. The Righi-Leduc voltage is also proportional to magnetic field, but not to external current.
7. **Misalignment voltage (V_M):** The excitation current flowing through the sample produces a voltage gradient parallel to the current flow. Even in zero magnetic field, a voltage appears between the two contacts used to measure the Hall voltage if they are not electrically opposite each other. Voltage contacts are difficult to align exactly. The misalignment voltage is frequently the largest spurious contribution to the apparent Hall voltage

The apparent Hall voltage, V_{Ha}, measured with a single reading contains all of the above spurious voltages: $V_{Ha} = V_H + V_o + V_S + V_E + V_N + V_R + V_M$.

All but the Hall and Ettingshausen voltages can be eliminated by combining measurements, as shown in Table B-1. Measurements taken at a single magnetic field polarity still have the misalignment voltage, frequently the most significant unwanted contribution to the measurement signal. Comparing values of Rh(+B) and Rh(-B) reveals the significance of the misalignment voltage relative to the signal voltage.

A Hall measurement is fundamentally a voltage divided by a current, so excitation current errors are equally as important. Current offsets, I_o, are canceled by combining the current measurements, then dividing the combined Hall voltage by the combined excitation current.

Table A-2 Hall effect measurement voltages showing the elimination of all but the Hall and Ettingshausen voltages by combining readings with different current and magnetic field polarities.

	I	B	V_H	V_M	V_S	V_E	V_N	V_R	V_O
V_1	+	+	+	+	+	+	+	+	+
V_2	–	+	–	–	+	–	+	+	+
$(V_1 – V_2)$			$2V_H$	$-2V_M$	0	$2V_E$	0	0	0
V_3	+	–	–	+	+	–	–	–	+
V_4	–	–	+	–	+	+	–	–	+
$(– V_3 + V_4)$			$2V_H$	$- 2V_M$	0	$2V_E$	0	0	0
$(V_1 – V_2 – V_3 + V_4)$			$4V_H$	0	0	$4V_E$	0	0	0

A.5.2 Geometrical Errors in Hall Bar Samples

Geometrical error sources in the Hall bar arrangement are caused by deviations of the actual measurement geometry from the ideal of a rectangular solid with constant current density and point-like voltage contacts.

The first geometrical consideration with the Hall bar is the tendency of the end contacts to short out the Hall voltage. If the aspect ratio of sample length to width *l / w* = 3, then this error is less than 1%.[15] Therefore, it's important $l / w \geq 3$.

The finite size of the contacts affects both the current density and electric potential in their vicinity, and may lead to fairly large errors. The errors are larger for a simple rectangular Hall bar than for one in which the contacts are placed at the end of arms.

For a simple rectangle, the error in the Hall mobility can be approximated (when μB << 1) by[16]

$$\frac{\Delta\mu_H}{\mu_H} = 1 - (1 - e^{-\pi l/2w})(1 - 2c/\pi w).$$

Here, $\Delta\mu_H$ is the amount μ_H must *increase* to obtain a true value.

If *l/w* = 3, and *c/w* = 0.2, then $\Delta\mu_H / \mu_H = 0.13$, which is certainly a significant error.

Reduce the contact-size error to acceptable levels by placing contacts at the ends of contact arms.[17] The following aspect ratios yield small deviations from the ideal: $p \approx c, c \leq w/3, l \geq 4w$.

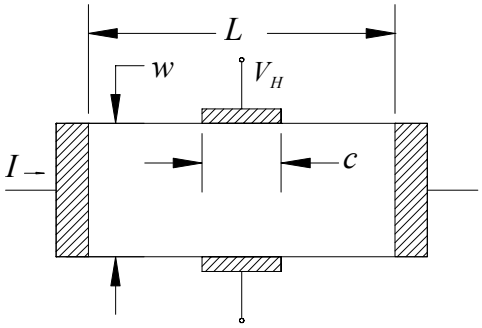

Figure A-7 Hall Bar With Finite Voltage Contacts

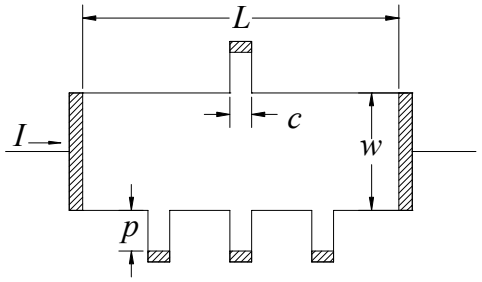

Figure A-8 Hall Bar With Contact Arms

A.5.3 Geometrical Errors in van der Pauw Structures

Van der Pauw's analysis of resistivity and Hall effect in arbitrary structures assumes point-like electrical connections to the sample. In practice, this ideal can be difficult or impossible to achieve, especially for small samples. The finite-contact size corrections depend on the particular sample geometry, and, for Hall voltages, the Hall angle θ (defined by $\tan\theta \cong \mu B$, where μ is the mobility). Look[2] presents the results of both theoretical and experimental determinations of the correction factors for some of the most common geometries. We summarize these results here, and compare the correction factors for a 1:6 aspect ratio of contact size to sample size.

A.5.3.1 Square Structures

The resistivity correction factor $\Delta\rho/\rho$ for a square van der Pauw structure is roughly proportional to$(c / l)^2$ for both square and triangular contacts. At (c / l) = 1/6, $\Delta\rho/\rho$ = 2% for identical square contacts, and $\Delta\rho/\rho$ < 1% for identical triangular contacts[18]. Hall voltage measurement error is much worse, unfortunately. The correction factor ΔR_H / R_H is proportional to (c / l), and is about 15% for triangular contacts when (c / l) = 1/6. The correction factor also increases by about 3% at this aspect ratio as the Hall angle increases from $\tan\theta$ = 0.1 to $\tan\theta$ = 0.5.

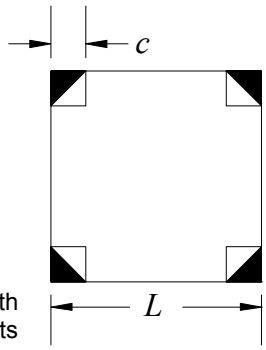

Figure A-9 Square van der Pauw Structure with Either Square or Triangular Contacts

A.5.3.2 Circular Structures

Circular van der Pauw structures fare slightly better. van der Pauw[14] gives a correction factor for circular contacts of

$$\frac{\Delta\rho}{\rho} \cong -\frac{1}{16\ln 2}\left(\frac{c}{l}\right)^2 \qquad \text{(per contact)},$$

which results in a correction of $\Delta\rho/\rho$ = -1% for (c / l) = 1/6 for four contacts. For the Hall coefficient, van der Pauw gives the correction

$$\frac{\Delta R_H}{R_H} \cong \frac{2}{\pi^2}\frac{c}{l} \qquad \text{(per contact)}.$$

At (c / l) = 1/6, this results in a correction of 13% for four contacts.

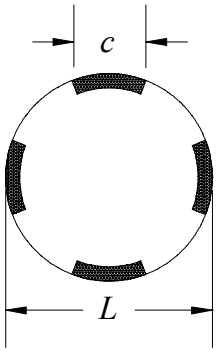

Figure A-10 Circular van der Pauw Structure

van Daal[19] reduced these errors considerably (by a factor of 10 to 20 for resistivity, and 3 to 5 for Hall coefficient) by cutting slots to turn the sample into a cloverleaf.

The clover leaf structure is mechanically weaker than the square and round samples unless it is patterned as a thin film on a thicker substrate. Another disadvantage is that the "active" area of the cloverleaf is much smaller than the actual sample.

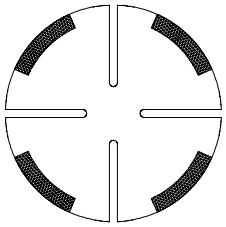

Figure A-11 Cloverleaf van der Pauw Structure

A.4.3.3 Greek Cross Structures

The Greek cross is one of the best van der Pauw geometries to minimize finite contact errors. Its advantage over simpler van der Pauw structures is similar to placing Hall bar contacts at the ends of arms. David and Beuhler[20] analyzed this structure numerically. They found that the deviation of the actual resistivity ρ from the measured value ρ_m obeyed

$$E = 1 - \frac{\rho}{\rho_m} = (0.59 \pm 0.006) \exp\left[-(6.23 \pm 0.02) \frac{a}{c} \right].$$

This is a very small error: for c / (c + 2a) = 1/6, where c + 2a corresponds to the total dimension of the contact arm, $E \cong 10^{-7}$.

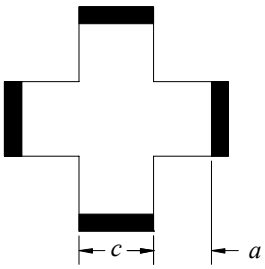

Figure A-12 Greek Cross van der Pauw Structure

Hall coefficient results are substantially better. De Mey[21,22] has shown that

$$\frac{\mu_H - \mu_{Hm}}{\mu_H} = \frac{\Delta\mu_H}{\mu_H} \cong 1.045 e^{-\pi a/c} \quad \text{(four contacts)},$$

where μ_H and μ_{Hm} are the actual and measured Hall mobilities, respectively. For c / (c + 2a) = 1/6, this results in $\Delta\mu_H / \mu_H \cong 0.04\%$, which is quite respectable.

References

[1] Schroder, D.K. Semiconductor Material and Device Characterization, John Wiley & Sons, New York (1990).

[2] Look, David C., Electrical Characterization of GaAs Materials and Devices, John Wiley & Sons, Chichester (1989).

[3] Meyer, J.R., Hoffman, C.A., Bartoli, F.J., D.A. Arnold, S. Sivananthan and J.P. Faurie, "Methods for Magnetotransport Characterization of IR Detector Materials", Semicond. Sci. Technol. (1993) 805-823.

[4] ASTM Standard F76-86, "Standard Method for Measuring Hall Mobility and Hall Coefficient in Extrinsic Semiconductor Single Crystals", 1991 Annual Book of ASTM Standards, Am. Soc. Test. Mat., Philadelphia (1991).

[5] Look, D. C. *et al.,* "On Hall scattering factors holes in GaAs", J. Appl. Phys., **80**, 1913 (1996).

[6] Chwang, R., Smith, B.J. and Crowell, C.R., "Contact size effects on the van der Pauw method for resistivity and Hall coefficient measurement", Solid-State Electron. **17** (Dec 1974) 1217-1227.

[7] Perloff, D.S., "Four-point probe sheet resistance correction factors for thin rectangular samples", Solid-State Electron. **20** (Aug 1977) 681-687.

[8] David, J.M. and Buehler, M.G., "A numerical analysis of various cross sheet resistor test structures", Solid-State Electron. **20** (Aug 1977) 539-543.

[9] Beck, W.A. and Anderson, J.R., "Determination of electrical transport properties using a novel magnetic field-dependent Hall technique", J. Appl. Phys. **62** 2 (Jul 1987) 541-554.

[10] Brugger, H. and Koser, H., "Variable-field Hall technique: a new characterization tool for JFET/MODFET device wafers", III-Vs Review, Vol. 8 No. 3 (1995) 41-45.

[11] Antoszewski, J., Seymour, D.J., Meyer, J.R., and Hoffman, C.A., "Magneto-transport characterization using quantitative mobility-spectrum analysis (QMSA)", Presented at: Workshop on the Physics and Chemistry of Merury Cadmium Telluride and Other IR Materials, 4-6 Oct. 1994, Alberqueque, NM, USA.

[12] ASTM Standard F76, American Society for testing and Materials, Philadelphia (1991).

[13] van der Pauw, L. J., "A method of measuring specific resistivity and Hall effect of discs of arbitrary shape", *Philips Res. Reports,***13**,1-9 (1958).

[14] ASTM Standard F76, American Society for testing and Materials, Philadelphia (1991).

[15] Volger, J. , "Note on the Hall potential across an inhomogeneous conductor", *Phys. Rev.,***79**,1023-24 (1950).

[16] Haeussler, J. and Lippmann, H., "Hall-generatoren mit kleinem Linearisierungsfehler", *Solid-State Electron.*,**11**,173-82 (1968).

[17] Jandl, S, Usadel, K.D., and Fischer, G., "Resistivity measurements with samples in the form of a double cross", *Rev. Sci. Inst.,***19**,685-8 (1974).

[18] Chwang, R., Smith, B.J., and Crowell, C.R., "Contact size effects in transition-metal doped semiconductors with application to Cr-doped GaAs", *J. Phys. C: Solid State Phys.,***13**, 2311-23 (1974).

[19] van Daal, H.J., "Mobility of charge carriers in silicon carbide", *Phillips research reports,* **Suppl. 3**,1-92 (1965).

[20] David, J.M. and Beuhler, M.G, "A numerical analysis of various cross sheet resistor test structures", *Solid State Electron..,* **20**, 539-43 (1977).

[21] De Mey, G., "Influence of sample geometry on Hall mobility measurements", *Arch. Electron. Uebertragungstech.,* **27**, 309-13 (1973).

[22] De Mey, G., "Potential Calculations for Hall Plates", *Advances in Electronics and Electron Physics, Vol. 61,* **(Eds. L. Marton and C. Marton), pp. 1-61, Academic, New York (1983**).

This Page Intentionally Left Blank